



# Computational Analysis of Integrated Engine Exhaust Nozzle on a Supersonic Fighter Aircraft

I. Arif<sup>1†</sup>, J. Masud<sup>2</sup> and I. Shah<sup>1</sup>

<sup>1</sup> Department of Aerospace Engineering, College of Aeronautical Engineering, National University of Sciences and Technology, H-12, Islamabad, Pakistan

<sup>2</sup> Department of Mechanical Engineering, Air University, Islamabad, Pakistan

†Corresponding Author Email: [arsalan\\_sayani@cae.nust.edu.pk](mailto:arsalan_sayani@cae.nust.edu.pk)

(Received March 14, 2018; accepted May 9, 2018)

## ABSTRACT

A unique approach of analyzing jet exhaust nozzle integrated to aircraft and propulsion system is presented in this paper. Engine exhaust nozzle is usually omitted in Wind Tunnel Testing and numerical analysis of aircraft due to complexities involved in integration of nozzle and presence of high pressure / temperature inside exhaust nozzle. Also, the flow properties are non-uniform and highly turbulent in the vicinity of nozzle. Therefore, exhaust nozzle is usually analyzed in isolation and these results often lead to inaccuracies from actual scenario where nozzle is integrated with aircraft and its propulsion system. This research aims to integrate engine exhaust nozzle on a supersonic fighter aircraft and analyze its flow characteristics and variation in performance parameters due to its integration. Engine propulsion characteristics and parameters such as nozzle inlet temperature and total pressure have been analyzed through an in-house validated engine analytical model developed by some of the authors of this study. In the first part of paper, exhaust plume structure has been analyzed to study the flow behaviour (flow turbulence and flow distortion etc) at nozzle exit. Later, nozzle performance parameters such as Exit Velocity, Nozzle Pressure Ratio (NPR), Engine Pressure Ratio (EPR), and Engine Temperature Ratio (ETR) have been calculated when exhaust nozzle is integrated with the aircraft. Finally, the results are compared and validated with analytical calculations to compare the performance of nozzle when it is in isolation and when it is integrated on aircraft. It is observed that nozzle flow has no significant effect on aircraft major surfaces such as fuselage, wing upper and lower surfaces, and nose section. However, there is a prominent effect of exhaust nozzle flow on horizontal stabilizers, vertical tail and rear fuselage area of the aircraft. An average difference of 18% in NPR, 12% in EPR, and 9% in ETR is observed between integrated nozzle and isolated nozzle which further signifies the importance of integrating exhaust nozzle in aircraft analysis. This proposed methodology will allow more accurate analysis of the effects of exhaust nozzle on the overall performance of aircraft. The methodology can further be used for proposing design changes in existing nozzle configurations.

**Keywords:** Aerodynamics; Internal Flows; Nozzle; Plume; Nozzle Pressure Ratio.

## NOMENCLATURE

$\alpha$	Angle of Attack	P	Static pressure (Pa)
$AoA$	Angle of Attack	$S-A$	One equation Spalart-Allmaras turbulence model
CFD	Computational Fluid Dynamics	RANS	Reynolds Averaged Navier-Stokes
Mach number	Mach number	$y^+$	Non-dimensional length scale associated with turbulence model
NPR	Nozzle Pressure Ratio		
EPR	Engine Pressure Ratio		
ETR	Engine Temperature Ratio		

## 1. INTRODUCTION

Engine exhaust nozzle is a simple yet sensitive device which allows the hot gasses to flow through it. Nozzle performance largely depends upon its

shape, size and location on aircraft. Exhaust nozzle integrates propulsion system with aircraft systems and its design is critical to engine performance (Boyce 2011). Its design includes installed and uninstalled performance estimation. Other design challenges include area variations through

convergent divergent principle, thrust vectoring and thrust reversing (Gamble, *et al.* 2004). Flow ingested into engine through intake or propelled through exhaust have a prominent effect on flow surrounding the body. Generally, analysis of exhaust nozzle is excluded from aircraft numerical analysis as it involves complexities related to internal flows and its interaction with external flow over the aircraft surface. Furthermore, integration of exhaust nozzle with aircraft requires comprehensive data about the installed propulsion system to evaluate boundary conditions for exhaust nozzle at each flight condition which is only available to manufacturers. However, this simplification and assumption often results in considerable inaccuracies in analysing the aircraft characteristics and nozzle performance as well. For any design engineer, it is critical to evaluate nozzle uninstalled and installed performance to accurately predict the aircraft performance.

A significant number of studies on exhaust nozzle design and its performance in isolation has been conducted in the past and available in literature (Rao 1958, Mikhail, *et al.* 1980, Stitt 1990, Li and Gutmark 2005, Jassim 2016, Viridi, *et al.* 2017). Many researchers studied the flow downstream of exhaust nozzle to analyze the jet plume structure (Mc Ghee 1970, Robinson and High 1974, DalBello, *et al.* 2004). Jet plume characteristics has been studied in detail by Korst, *et al.* and Adamson Jr. (Korst, *et al.* 1981, Adamson Jr 2012). Similarly, computational analysis of exhaust plumes of axisymmetric nozzle was performed to analyze the jet plume characteristics (Dash, *et al.* 1978, DalBello, *et al.* 2004). The study conducted by Dash *et al.* included shock structure, viscous and shear effects and mixing effects of jet (Dash, *et al.* 1978). Later, a parabolized Navier-Stokes model was developed to simulate the viscous flow (Dash, *et al.* 1985). The model was found to be quite compatible in analyzing the effect of viscous flow turbulent jet mixing. Chuech, *et al.* (Chuech, *et al.* 1989) modified the k-epsilon turbulence model to study the turbulent mixing phenomena in under expanded jet flow in stagnant medium. Later, the k-epsilon model was further modified to analyze the compressibility effects at high speed. This model yielded much better results to predict the pressure at different points in under expanded nozzle. A two equation k-epsilon model was successfully applied to predict the jet flow of under-expanded nozzle using Reynolds Averaged Navier Stokes Equations (RANS) (Woodmansee, *et al.* 1999). This model allowed to ascertain the Mach number upstream of Mach disc and yielded accurate results in agreement with experimental data.

Though a significant literature is available on jet nozzle design, characteristics and performance. However, most of the research on exhaust nozzle flows are done with jet exhaust nozzle in isolation or their associated base flows (Rao 1958, Mikhail, *et al.* 1980, Abdol-Hamid, *et al.* 1993, Li, *et al.* 2009, Butt and Arshad 2015). These studies mainly focused on flow behavior inside and downstream of exhaust nozzle, whereas, the actual nozzle flow

characteristics and performance is quite different when propulsion system and aircraft external flow interaction with exhaust plume is taken into account. Effect of jet exhaust plume on control surfaces of aircraft and change in pitching and yawing moments are also important in determining the stability parameters of aircraft (Pandya, *et al.* 2004).

A unique approach of analyzing jet exhaust nozzle integrated to aircraft and propulsion system is presented in this paper. Internal flow through exhaust nozzle interacts with external flow over the aircraft and plume structure is observed which is different than the plume structure observed downstream of a nozzle in isolation. Engine propulsion characteristics and parameters such as nozzle inlet temperature and total pressure were analyzed through an in-house developed engine analytical model developed by some of the authors of this study (Arif, *et al.* 2018).

Owing to the complexities involved in the integrated solution of internal and external flows, previous numerical studies on the selected aircraft did not consider aircraft propulsion system and exhaust nozzle while carrying out flow simulations around the aircraft (Hassan, *et al.* 2015). Separate analysis of propulsion system have however, been conducted (Arif, *et al.* 2018). In order to integrate the propulsion system and exhaust nozzle with baseline aircraft for numerical analysis, it was important to ascertain different engine parameters at all flight conditions. Calculation and finalization of boundary conditions is considered one of the most critical step in CFD analysis. Input conditions for intake, exhaust and aircraft were required for each flight condition in order to carry out accurate numerical analysis. Calculation of exhaust nozzle boundary conditions is quite complex and cumbersome as it requires complete details of propulsion system. For this purpose, mathematical modelling for RD-93 engine was carried out to ascertain the exhaust nozzle boundary conditions (pressure, temperature, pressure ration etc) at different flow conditions.

The analysis in this research is carried out at subsonic and supersonic regimes at different flight conditions. The final geometry includes exhaust nozzle and intake duct along with aircraft external surfaces. The paper is divided into two major parts, the first part presents the exhaust flow characteristics observed plume structure downstream of exhaust nozzle when it is integrated with aircraft. Exhaust plume structure is analyzed to observe the flow behavior (flow turbulence and flow distortion) at nozzle exit. In the second part, nozzle performance is analyzed when it is integrated with the aircraft. Nozzle performance parameters such as Exit Velocity, Nozzle Pressure Ratio, Engine Pressure Ratio, and Engine Temperature Ratio are calculated for comprehensive analysis. Finally, the results are compared and validated with analytical calculations to compare the performance of nozzle when it is in isolation and when it is integrated on aircraft. The aircraft and exhaust nozzle geometries are shown in Fig. 1 below.

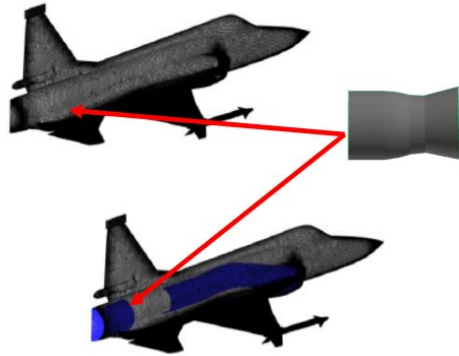


**Fig. 1. Aircraft without exhaust nozzle (Top) and with exhaust nozzle (Bottom)**

## 2. MODELLING AND COMPUTATIONAL SETUP

During the course of research, number of steps were followed which commenced from exhaust nozzle modelling and integrating it with aircraft and intake geometries. Aircraft, intake and exhaust were taken as separate entities so that changes can be made in any of the part without affecting other geometry. Exhaust geometry was modelled with the help of dimensions provided by Manufacturer’s engine manual. The geometries were meshed and were later appended to Numerical Solver Software Fluent® (ANSYS 2013). The meshing strategy adopted for the research was based on unstructured scheme for all geometries including aircraft, intake and exhaust.

Numerical simulations were carried out at zero side slip angle which allowed the simulation with symmetry plane. For numerical analysis in this study, Reynolds-averaged Navier-Stokes (RANS) set of equations are used to account for time dependent behavior of flow. The governing conservation equations are (Hirsch 2007):

Conservation of Mass:

$$\frac{\partial \rho}{\partial t} + \frac{\partial(\rho u)}{\partial x} + \frac{\partial(\rho v)}{\partial y} + \frac{\partial(\rho w)}{\partial z} = 0 \quad (1)$$

Conservation of Momentum:

$$\rho \left( \frac{\partial u}{\partial t} + u \frac{\partial u}{\partial x} + v \frac{\partial u}{\partial y} + w \frac{\partial u}{\partial z} \right) = -\frac{\partial p}{\partial x} + \mu \left( \frac{\partial^2 u}{\partial x^2} + \frac{\partial^2 u}{\partial y^2} + \frac{\partial^2 u}{\partial z^2} \right) + F_x \quad (2)$$

$$\rho \left( \frac{\partial v}{\partial t} + u \frac{\partial v}{\partial x} + v \frac{\partial v}{\partial y} + w \frac{\partial v}{\partial z} \right) = -\frac{\partial p}{\partial y} + \mu \left( \frac{\partial^2 v}{\partial x^2} + \frac{\partial^2 v}{\partial y^2} + \frac{\partial^2 v}{\partial z^2} \right) + F_y \quad (3)$$

$$\rho \left( \frac{\partial u}{\partial t} + u \frac{\partial u}{\partial x} + v \frac{\partial u}{\partial y} + w \frac{\partial u}{\partial z} \right) = -\frac{\partial p}{\partial x} + \mu \left( \frac{\partial^2 u}{\partial x^2} + \frac{\partial^2 u}{\partial y^2} + \frac{\partial^2 u}{\partial z^2} \right) + F_x \quad (4)$$

Conservation of Energy:

$$\rho C_p \left( \frac{\partial T}{\partial t} + u \frac{\partial T}{\partial x} + v \frac{\partial T}{\partial y} + w \frac{\partial T}{\partial z} \right) = \Phi + \frac{\partial}{\partial x} \left[ k \frac{\partial T}{\partial x} \right] + \frac{\partial}{\partial y} \left[ k \frac{\partial T}{\partial y} \right] + \frac{\partial}{\partial z} \left[ k \frac{\partial T}{\partial z} \right] \quad (5)$$

where,

$\rho$  is the fluid density;  $\mu$  is the kinematic viscosity;  $u, v, w$  are the component of velocity in Cartesian coordinates;  $p$  is the pressure term;  $F_x, F_y, F_z$  are the body force terms;  $T$  is temperature in Kelvins; and  $k$  is the heat transfer coefficient.

### 2.1 Overview of Engine Modelling

The propulsion system of the aircraft under study is a dual-duct, dual-rotator turbofan engine, which has an afterburner shared by inner/outer channel and a fully adjustable supersonic nozzle. Due to military confidentiality, comprehensive engine performance data of fighter aircraft engines at different operating conditions is not available with its users. Hence, it is impossible to ascertain certain flow parameters such as pressure and temperature at different engine stations or propose any design modification in existing engine design. In order to determine the flow properties at certain engine components specially exhaust nozzle for further numerical analysis of aircraft with integrated propulsion system, an in-house analytical model was developed and validated at Afterburner configuration (Arif, *et al.* 2018). A comprehensive scheme was developed for modelling and simulation engine in accordance with Aircraft Engine Design literature (Mattingly 2002) and software packages ONX® and PERF®. The model is verified by thrust matching technique which further helped in ascertaining different engine parameters at off design conditions as well. This analytical model also forms an important part of an already conducted and published study by the same authors for characterization of exhaust effects on aerodynamic behavior of a supersonic aircraft (Masud, *et al.* 2017).

### 2.2 Grid Density

Computational grid size and type plays an important part in computational analysis. The grid generation must be fine enough to resolve all flow gradients. However, this aspects needs to be balanced with available computational power which puts limit on grid size. Aircraft and exhaust geometries were meshed separately using unstructured meshing scheme. Tetrahedral mesh generated for aircraft and domain cannot capture the near wall effects for a reasonable mesh size. For this purpose, a five layer

prism was applied on aircraft boundary to accurately capture boundary layer and near wall effects. A very dense mesh was created in exhaust plume area to analyze the flow behavior downstream of exhaust. Turbulent  $y^+$  values were kept at optimum level for different flight speeds. Prime importance was given to mesh consistency with previous research (Masud, *et al.* 2017) to validate and compare the results.

### 2.3 Grid Independence

Size and type of grid has significant impact on the accuracy of results. A highly dense and fine mesh can achieve high accuracy but it is usually computationally expensive in terms of time and resources. Hence, it is important to maintain a balance between the generated size of mesh and accuracy of results achieved. In order to select an optimum mesh size, a grid independence study was carried out before the final selection of mesh. Three different meshes were generated based on the number of cells and size function. Nozzle Pressure Ratio at Mach number. 0.6 and AoA  $0^\circ$  for each mesh was evaluated for comparative analysis. Details of mesh are presented in following Table 1 and results are shown in Fig. 2 below.

**Table 1 Grid Independence Analysis**

Grid	Cells
Grid 1	8.9 million
Grid 2	11.2 million
Grid 3	13.3million

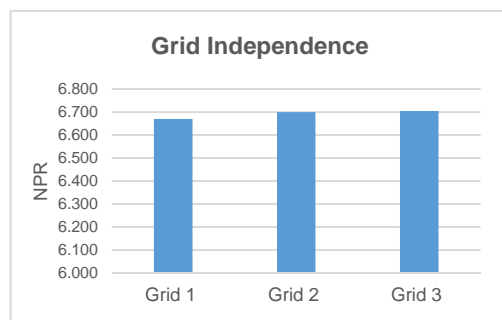


**Fig. 2. Grid Independence Study**

It was observed that variation in Nozzle Pressure Ratio was almost negligible for Grid 2 (11.2 million) and Grid 3 (13.3 million), however, for Grid 1, Nozzle Pressure Ratio was under predicted. Based on this grid independence study, a Grid 2 (11.2 million) was selected for further analysis (shown in Fig. 3).

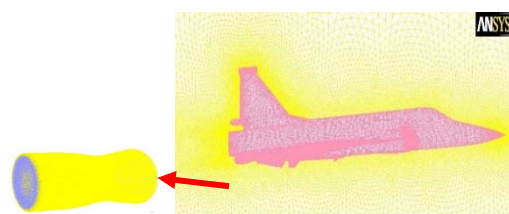


**Fig. 3. Final Meshed Geometries of Aircraft and Exhaust Nozzle**

### 2.4 Solution Strategy

For numerical analysis, Reynolds-Averaged Navier-Stokes (RANS) set of equations are used to account for time dependent behavior of flow. Double precision solver was used for better accuracy and fluid was taken as air with ideal gas properties. Density based solver was selected with explicit algorithm. Due to sensitivity and importance of temperature effects in the research, energy equation option was also used. 2nd order upwind scheme was selected in flow discretization and 1st order upwind scheme was used to cater for turbulent viscosity. Suitable relaxation parameters were applied and a courant number of 1 was selected (Masud, *et al.* 2017).

### 2.5 Boundary Conditions

All surfaces of aircraft were selected as no slip walls. Input conditions for exhaust and aircraft were calculated separately for this research. The evaluation of boundary conditions at exhaust nozzle was a complex task as it required complete analysis of propulsion system. For this purpose, a complete analytical model of engine was developed and validated with manufacturer's provided data by some of the authors of this study (Arif, *et al.* 2018). For all Mach number (subsonic and supersonic), static pressures values were taken in accordance with atmospheric sea level conditions. The case was analyzed at subsonic and supersonic Mach number with varying angles of attack and mass flow rates. Design mass flow rate is set as 44 kg/s, 50 kg/s and 105 kg/s for Mach numbers 0.6, 0.8 and 1.5 respectively. Whereas, off design mass flow rate is set as 30 kg/s, 40 kg/s and 90 kg/s for Mach numbers 0.6, 0.8 and 1.5 respectively.

### 2.6 Turbulence Model Independence

Selection of turbulence model is as important as selection of grid size for numerical analysis, hence, this aspect cannot be ignored. For this research, three different models (SA, k-epsilon and k-omega) were analyzed keeping in view the complex flow phenomenon involving both internal flow inside exhaust nozzle and external flow over aircraft. SA is a single equation turbulence model while k-epsilon and k-omega are two equation turbulence models (Kuntz and Menter 2004, Bulat and Bulat 2013). Comparative results of NPR for these models are presented in Fig. 4 below:

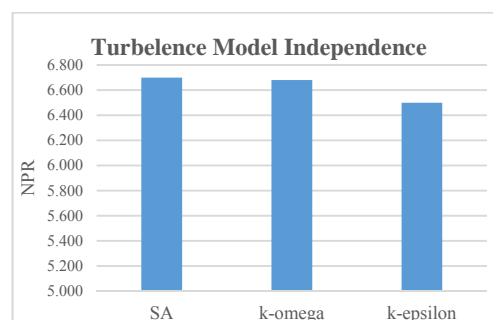


**Fig. 4. Turbulence Model Independence**

Based on the results, it was observed that the variation between the NPR obtained from S-A model and k-omega model was almost negligible, however, the results obtained from k-epsilon were slightly under predicted. The convergence stability and residuals from S-A and k-epsilon were not satisfactory as disordered sinusoidal behavior was observed throughout the simulations. Hence, the average of last 1000 iterations were taken into account for estimation of NPR. Hence, k-omega turbulence model was selected for this research based on the accuracy of results and its convergence stability. K-omega is a two equation turbulence model which includes extra transport equations to evaluate turbulent properties of fluid (2016). The results were consistent and in agreement with previous research (Hassan, *et al.* 2015, Masud, *et al.* 2017).

### 3. ANALYSIS OF FLOW CHARACTERISTICS

The analysis was carried out at three different Mach numbers (0.6, 0.8 and 1.5) at five different angle of attack (-4, 0, 4, 8, 12). Analysis on calculated results is divided into two parts, namely, Flow Characteristics Downstream of Exhaust and Exhaust Nozzle Performance Analysis. Flow characteristics including turbulence, plume structure, and pressure distribution at different flight conditions are observed and are presented in subsequent sections.

#### 3.1 Pressure Distribution

The analysis at subsonic speeds was carried out at two different Mach numbers, i.e. 0.6 and 0.8, whereas the supersonic analysis was carried out at Mach number 1.5. Pressure contours at Mach numbers 0.6, 0.8 and 1.5 are shown in Fig. 5:

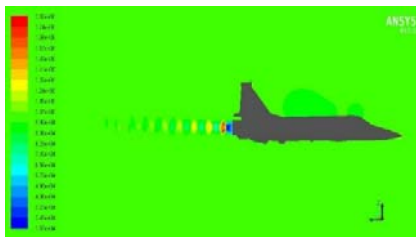


Fig. 5a. Pressure Contours at Mach number 0.6 AoA 0

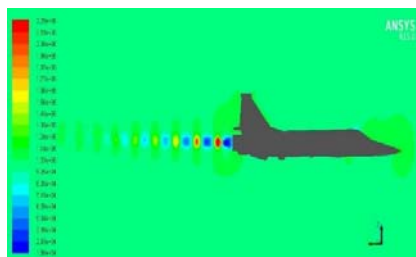


Fig. 5b. Pressure Contours at Mach number 0.8 AoA 0



Fig. 5c. Pressure Contours at Mach number 1.5 AoA 0

Pressure contours on aircraft and flow downstream of exhaust nozzle is clearly visible in the Figs. 5a, b and c. At subsonic Mach numbers, a large plume section can be observed downstream of exhaust nozzle in the form of shock waves and expansion waves. From the plume structure, it is clearly evident that the nozzle is under expanded for all flow conditions. From the pressure distribution contours at subsonic flow, it is observed that nozzle flow has no significant effect on aircraft major surfaces such as fuselage, wing upper and lower surfaces, and nose section. However, there is a prominent effect of exhaust nozzle flow on horizontal stabilizers, vertical tail and rear fuselage area of the aircraft. Variation in NPR at different Mach numbers are shown in Table 2 below.

Table 2 Nozzle Pressure Ratio Variation with Mach number

M #	NPR
0.6	6.6
0.8	6.72
1.5	6.80

From the table above, it can be observed that with an increase in Mach number, nozzle pressure ratio slightly increases from 6.6 to 6.8, which shows that the nozzle becomes more under expanded with increase in speed. This is due to fact that the pressure at the exit of nozzle is unable to expand till free stream pressure, hence the exit pressure is higher than free stream pressure at that particular flow condition (Mattingly and Von Ohain 2006).

In supersonic flow, the plume section is not clearly visible due to excessive pressures in surroundings due to presence of shock waves. Although, the nozzle is still under expanded but the pressure gradients due to shock structure dominates the flow. Formation of strong shock waves are dominant in pressure contours on aircraft nose, fuselage and wing area. However, at supersonic speeds, a plume structure can be clearly observed if temperature plots are generated.

#### 3.2 Flow Characteristics Inside the Nozzle

Flow behavior inside the exhaust nozzle was studied to analyze whether the nozzle is perfectly expanded, under-expanded or over-expanded in test flight conditions. A sectional view and plot of static pressure variation along the length of nozzle at Mach number 0.8 is shown in Fig. 6 below.

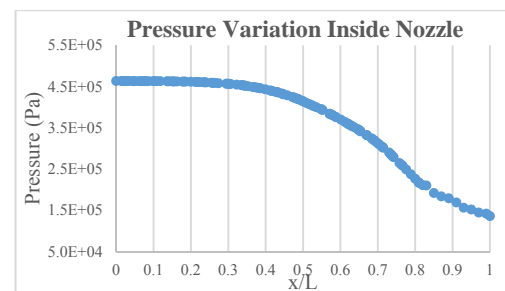


Fig. 6. Pressure Variation inside Nozzle

From pressure plot, it can be observed that the static pressure at the inlet of nozzle is quite high and slightly decreases till throat area, however, from throat area till exit of nozzle there is a sharp decrease in pressure which indicates sudden expansion and rise in flow velocity. However, the expansion of flow is not enough to match the atmospheric pressure at nozzle exit which indicates that the nozzle is under-expanded at this flight condition. Since the nozzle is under-expanded in this case, there is a certain loss in thrust potential of engine.

### 3.3 Flow Characteristics Downstream of Nozzle (Plume Structure)

Plume structure downstream of exhaust was studied in detail during the research. Jet plume structure at Mach number 0.8 at AoA 0° is shown in Fig. 7 below.

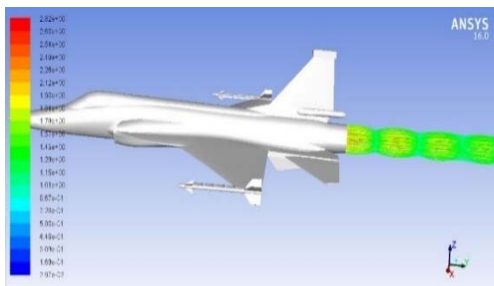


Fig. 7a. Plume Structure Downstream of Nozzle

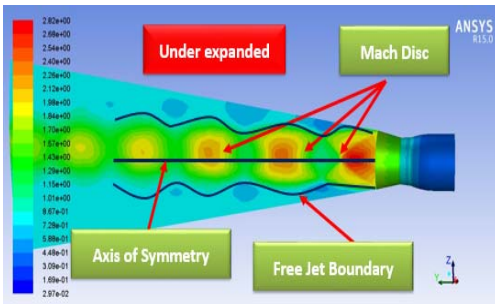


Fig. 7b. Plume Structure Velocity Contour at Mach number. 0.8

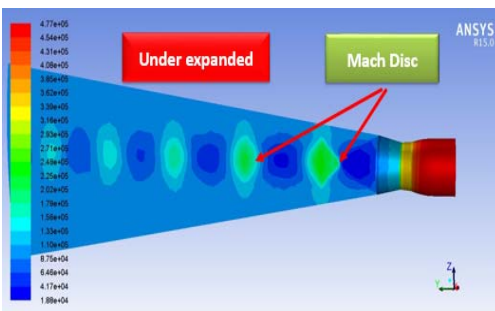


Fig. 7c. Plume Structure Pressure Contour at Mach number. 0.8

A typical jet plume phenomenon downstream of under-expanded nozzle can be seen in figure above. The horizontal line is the axis of symmetry of exhaust. The flow at the nozzle lip is deflected through an angle to expand the gas into free stream pressure. Inside the jet flow, the flow is expanded rapidly and causes the pressure to fall below

ambient pressure, hence compression waves are formed to increase the pressure upto ambient pressure. Compression waves are formed at the interaction of expansion waves with jet boundary. Merging of compression waves results in barrel shock. Barrel shock is the separation line between the region inside the plume which is independent of the ambient pressure and the region outside the plume which is dependent upon ambient pressure. Also, the expansion waves forming at the nozzle lips allows the gas velocity to increase which sweeps the barrel shock further away from nozzle axis. From the contours, Mach discs can be easily observed downstream of exhaust which are formed due to shock interactions. Also, jet boundary pattern and Mach discs are also clearly visible from the contour plot.

The variation of flow along the centreline of nozzle and downstream of nozzle is plotted in Fig. 8 to observe the flow behaviour inside and downstream of nozzle in combination.

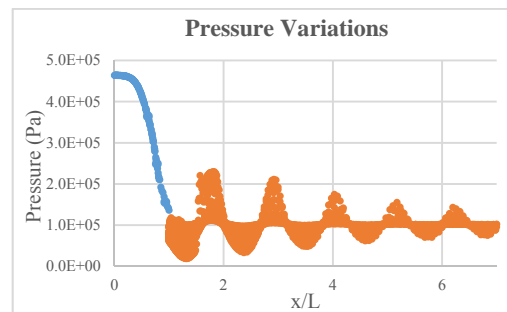


Fig. 8. Pressure Variations inside and downstream of Nozzle

From pressure plot, it is clearly evident that the flow pressure keeps decreasing inside the nozzle. However, the expansion of flow is insufficient and nozzle behaviour is under-expanded as pressure at nozzle exit is well above the ambient pressure. In this case, a complex jet plume is produced consisting of regions of decreasing and increasing pressure (or density) (Saddington, *et al.* 2004). Since the flow is viscous in nature, turbulent mixing and viscous losses with surrounding air causes the sinusoidal wave pattern to decay after small number of shock and expansion wave formations (Abbett 1971). This phenomenon can be observed by the sinusoidal variation in pressure plot. A mean centreline could also be observed through the plot and number of Mach discs formed due to under-expansion are also calculated with the help of the pressure plot. Same phenomenon can also be seen in Fig. 9 below:

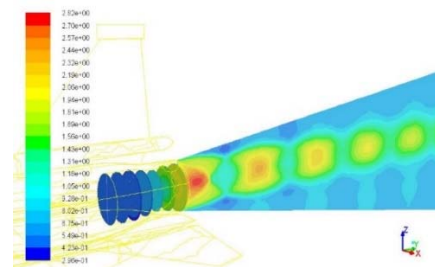


Fig. 9. Flow Structure inside and downstream of Nozzle

#### 4. EXHAUST NOZZLE PERFORMANCE ANALYSIS

The performance of exhaust nozzle is critical in overall efficiency of engine and the flow behaviour inside and downstream of exhaust. This section presents the exhaust nozzle characteristics under different conditions. In this part of research, nozzle performance is analyzed when it is integrated with the aircraft. The complete aircraft geometry included exhaust nozzle and intake duct along with aircraft external surfaces. Nozzle performance was predicted with high accuracy which was verified through the results and a plume structure was observed. Some of the most important parameters which identifies the nozzle performance includes Exit Jet Velocity, Nozzle Pressure Ratio (NPR), Engine Pressure Ratio (EPR), and Engine Temperature Ratio (ETR).

##### 4.1 Nozzle Pressure Ratio (NPR)

Nozzle pressure ratio (NPR) is the ratio of nozzle exit total pressure to static pressure. NPR of nozzle in isolation can be analytically calculated using the following expression (Mattingly and Von Ohain 2006).

$$NPR = P_{total\ exit} / P_{static\ exit} \quad (6)$$

The calculated values of NPR from numerical analysis and analytical calculations were plotted at different Mach number is shown in Fig. 10 below:

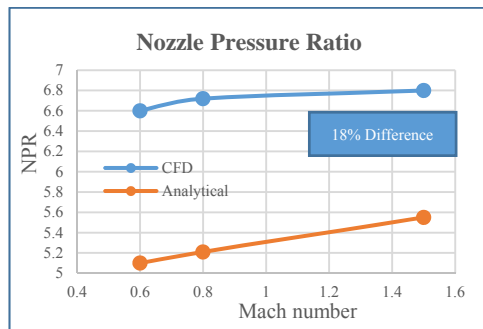


Fig. 10. Nozzle Pressure Ratio

From the Fig. 10, it is observed that at subsonic speeds, nozzle pressure ratio does not change, since the total pressure at the exit vary linearly with speed. Hence, the ratio of total pressure at exit to static pressure remains constant. However, at supersonic speed there is a slight increase in NPR. This is due to the fact that total pressure is governed by exit velocity which is more dominant in supersonic regime than in subsonic speeds. Therefore, the nozzle pressure ratio at supersonic speed is higher than subsonic speeds. A significant change in appearance of external flow field is also observed near the nozzle area in supersonic case as compared to subsonic case for the same NPR. There is a less dominant formation of shock and expansion waves near the exit as compared to subsonic Mach number. This aspect results in the increase of NPR, as the increase in freestream velocity has equivalent effect on NPR. Variation of NPR, EPR and ETR at Mach number 0.6 with change in AoA is shown in Table 3 below.

Table 3 Variation of NPR, EPR and ETR with change in AoA

M #	AoA	NPR	EPR	ETR
0.6	0	6.60	3.25	6.46
0.6	4	6.61	3.26	6.46
0.6	8	6.60	3.28	6.47
0.6	12	6.61	3.26	6.46
0.6	-4	6.61	3.25	6.47

It is observed that the NPR, ETR and EPR does not change with varying AoA. This is due to the fact that the inlet duct is able to deliver the design mass flow rate at all AoA effectively. This in turn keeps the engine operations normal at all AoA. Hence, NPR, ETR and EPR are not much effected by the change in AoA.

The nozzle pressure ratio calculated from CFD analysis was differs slightly from analytical results. An average difference of 18% was observed between the results at all flow conditions. The variations between the results are due to the fact that the analytical calculations are based on perfectly expanded nozzle, whereas from the CFD analysis it is evident that the nozzle is under expanded at these flight conditions. The magnitude of thrust loss due to under expansion in the exhaust nozzle cannot be estimated with analytical equations which results in slight deviation from actual results. Hence, results from numerical analysis using this methodology proved to be quite effective and realistic as it approximates the under expansion in actual scenario at these flight conditions.

##### 4.2 Engine Pressure Ratio (EPR)

Engine pressure ratio is the ratio of total pressure at exit to total pressure at compressor inlet. This parameter is directly dependent on engine performance and therefore does not depend on free stream pressure. Also, pressure losses in aircraft intake are not catered in engine pressure ratio. EPR of nozzle in isolation can be analytically calculated using the following expression (Mattingly and Von Ohain 2006).

$$EPR = P_{total\ exit} / P_{total\ compressor} \quad (7)$$

The calculated values of EPR from numerical analysis and analytical calculations were plotted at different Mach number is shown in Fig. 11 below:

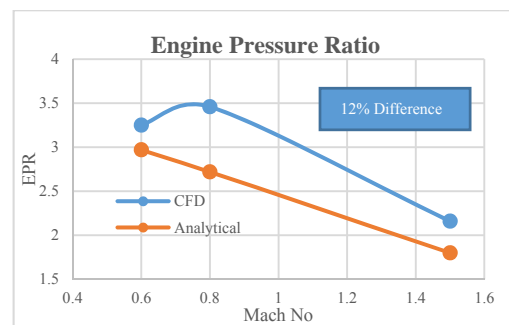


Fig. 11. Engine Pressure Ratio

At subsonic speeds, numerical analysis results show that EPR slightly increases from Mach number 0.6 to 0.8, whereas EPR calculated with analytical methodology slightly decreases. This variation is due to the fact that the analytical model is based on ideal expansion of nozzle and cannot predict the extent of under expansion or over expansion of flow through nozzle. A significant change in EPR was observed in supersonic case as compared to subsonic case for the same NPR. There was a less dominant formation of shock and expansion waves near the exit as compared to subsonic Mach number. It is observed that there is a large decrease in EPR at supersonic speeds. Due to formation of shock waves near aircraft nose, fuselage, wing and intake area, there is significant pressure change at these surfaces. Similarly, the total pressure at compressor inlet is also higher as compared to total pressure at compressor inlet at subsonic speeds. The Total Pressure at nozzle exit also increases but to a smaller extent as compared to the Total Pressure at compressor inlet.

The variation in calculated values of engine pressure ratio (EPR) is less than that of NPR. An average difference of 12% was observed between the results at all flow conditions. A reduction in difference between the two results was due to the fact that compressor total pressure can be estimated accurately at compressor inlet at design mass flow rate. Hence the impact of nozzle exit conditions for the calculation of engine pressure ratio is less than that for nozzle pressure ratio.

### 4.3 Engine Temperature Ratio (ETR)

Engine Temperature Ratio (ETR) is the ratio of nozzle total temperature to compressor inlet total temperature. ETR of nozzle in isolation can be analytically calculated using the following expression (Mattingly and Von Ohain 2006).

$$ETR = T_{total\ exit} / T_{total\ compressor} \quad (8)$$

The calculated values of ETR from numerical analysis and analytical calculations were plotted at different Mach number as shown in Fig. 12 below:

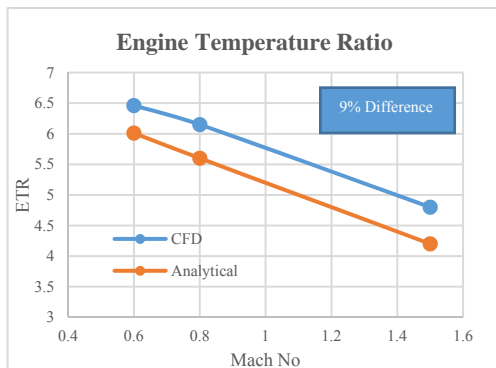


Fig. 12. Engine Temperature Ratio

From Fig. 12, it is observed that at subsonic speeds, engine temperature ratio slightly decreases from Mach number 0.6 to Mach number 0.8. This is due to the fact that the temperature limit is dependent

upon material limitations as well. Therefore, temperature at combustion chamber, turbine and afterburner section is dependent upon material temperature limit. This aspect limits the ETR to a certain value and hence only a slight decrease in ETR is observed at subsonic speeds. However, at supersonic speed, a significant decrease in EPR is observed as compared to subsonic speeds. Due to formation of shock waves near aircraft nose, fuselage, wing and intake area, there is significant temperature gradient at these surfaces. Similarly, the total temperature at compressor inlet is also higher as compared to total temperature at compressor inlet at subsonic speeds. The Total temperature at nozzle exit is restricted due to material temperature limitations and hence, the ratio decreases.

The variation in calculated values of engine temperature ratio (ETR) is also less than that of NPR. An average difference of 9% was observed. A reduction in difference between the two results was due to the fact that temperatures at combustion chamber, turbine and afterburner duct are restricted by material limitations. Hence the analytical results are in good agreement with CFD results.

### 4.4 Exit Velocity Calculations

Velocity calculations from CFD results along with comparison with analytical results are presented in this section. The exit velocity for a convergent-divergent nozzle can be evaluated by following expressions (Mattingly and Von Ohain 2006).

$$\frac{F_{ideal}}{A_8 P_t} = \frac{\gamma P_9 A_9 M_9}{P_t A_8} + \left( \frac{P_9}{P_t} - \frac{P_{amb}}{P_t} \right) \frac{A_9}{A_8} \quad (9)$$

and

$$F = \frac{\dot{m}_c}{g_c} (V_9 - V_0) + \frac{\dot{m}_F}{g_c} (V_{19} - V_0) \quad (10)$$

$$V_e = \sqrt{\frac{TR}{M} \cdot \frac{2\gamma}{\gamma-1} \cdot \left[ 1 - \left( \frac{p_e}{p} \right)^{\frac{\gamma-1}{\gamma}} \right]} \quad (11)$$

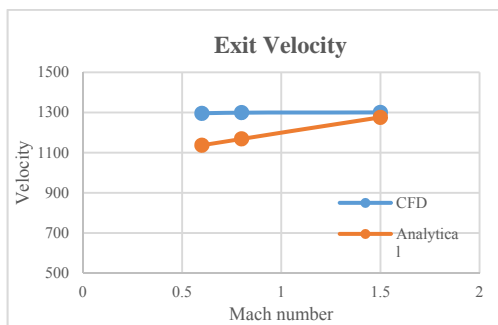
Comparison between calculated values of exit velocity with analytical calculations are presented in Table 4 below. A percentage difference of 10% was observed between the CFD calculation and analytical calculation at subsonic Mach number whereas the difference reduced to only 2% at supersonic flow condition.

Table 4 Comparative Analysis of Velocity

M #	Exit Velocity (CFD) (m/s)	Exit Velocity (Analytical) (m/s)	Percent Difference (%)
0.6	1296.1	1136.9	14.0 %
0.8	1299.48	1168.7	11.2 %
1.5	1300.43	1276.1	1.9 %

Variation in exit velocity at different flight speeds

for CFD and analytical results are shown in Fig. 13.



**Fig. 13. Comparative Analysis of Thrust Variation**

From the CFD results, it is observed that the exit velocity almost remains constant at all Mach number. This is due to the fact that the nozzle is under expanded at all flow conditions and pressure at nozzle exit remains higher than ambient pressure. However, exit velocity from analytical calculations increases when Mach number is increased as these calculations are carried out for perfectly expanded nozzle.

## 5. CONCLUSION

We have presented a unique approach of analyzing jet exhaust nozzle integrated to aircraft and propulsion system. The methodology requires external flow analysis over the aircraft, internal flow analysis inside exhaust nozzle and determination of boundary conditions at nozzle through analysis of propulsion system. A case of supersonic aircraft with integrated exhaust nozzle was analyzed using the same methodology. Flow characteristics of exhaust nozzle were analyzed and jet plume structure was studied / validated with literature. The propulsion system of the aircraft under study is a dual-duct, dual-rotator turbofan engine, which has an afterburner shared by inner/outer channel and a fully adjustable supersonic nozzle. In order to determine the flow properties at certain engine components specially exhaust nozzle for further numerical analysis of aircraft with integrated propulsion system, an in-house analytical model was developed and validated. The analysis was divided into two major parts. In the first part, flow characteristics inside and downstream of nozzle were studied. Later, nozzle performance was evaluated, compared and validated with nozzle performance in isolation.

It is observed that nozzle flow has no significant effect on aircraft major surfaces such as fuselage, wing upper and lower surfaces, and nose section. However, there is a prominent effect of exhaust nozzle flow on horizontal stabilizers, vertical tail and rear fuselage area of the aircraft. The results revealed that the nozzle under study was under-expanded at all test conditions. At the nozzle lip, flow deflected through an angle to expand the gas into free stream pressure. Compression waves were also formed at the interaction of expansion waves with jet boundary. Merging of compression waves resulted into barrel shock and Mach Discs. These phenomenon were observed through pressure plots

and pressure contours. Nozzle performance was predicted with high accuracy which was verified through the results and plume structure observed. A difference of 18% in NPR, 12% in EPR, and 9% in ETR was observed between integrated nozzle and isolated nozzle which further signifies the importance of integrating exhaust nozzle in aircraft analysis. The magnitude of thrust loss due to under expansion in the exhaust nozzle cannot be estimated with analytical equations, which results in slight deviation from actual results. Hence, numerical analysis results using this methodology proved to be quite effective and realistic as it approximates the magnitude of under expansion in actual scenario at these flight conditions.

## ACKNOWLEDGEMENTS

The authors acknowledge the use of Numerical Analysis Lab (NAL) of College of Aeronautical Engineering, Risalpur, Pakistan.

## REFERENCES

- ANSYS (R) (2016) from <http://www.ansys.com/Products/Fluids/ANSYS-Fluent>.
- Abbett, M. (1971). Mach disk in underexpanded exhaust plumes. *AIAA Journal* 9(3), 512-514.
- Abdol-Hamid, K. S., K. Uenishi, B. Keith and J. R. Carlson (1993). Commercial turbofan engine exhaust nozzle flow analyzes. *Journal of propulsion and power* 9(3), 431-436.
- Adamson Jr, T. (2012). On the structure of jets from highly underexpanded nozzles into still air. *Journal of the Aerospace sciences*, AIAA, Vol 1.
- ANSYS, I. (2013). CFD User's Manual. Ansys Inc.
- Arif, I., J. Masud, Z. G. Toor, S. Salamat and A. Javed (2018). *Analytical Modelling and Validation of RD-93 Turbofan Engine at Design Conditions*. AIAA Aerospace Sciences Meeting.
- Boyce, M. P. (2011). Gas turbine engineering handbook, Elsevier, 4<sup>th</sup> Edition. ISBN: 9780123838438.
- Bulat, M. P. and P. V. Bulat (2013). Comparison of turbulence models in the calculation of supersonic separated flows. *World Applied Sciences Journal* 27(10), 1263-1266.
- Butt, A. H. and A. Arshad (2015). *Design and analysis of a clustered nozzle configuration and comparison of its thrust*. Student Res. Paper Conf.
- Chuech, S., M. C. Lai and G. Faeth (1989). Structure of turbulent sonic underexpanded free jets. *AIAA Journal* 27(5), 549-559.
- DalBello, T., N. J. Georgiadis, D. A. Yoder and T. G. Keith (2004). Computational study of axisymmetric off-design nozzle flows. *AIAA paper* 530.

- Dash, S., H. Pergament and R. Wilmoth (1978). Prediction of nearfield jet entrainment by an interactive mixing/afterburning model. *AIAA Paper* 78-1189.
- Dash, S. M., D. E. Wolf and J. Seiner (1985). Analysis of turbulent underexpanded jets. I-Parabolized Navier-Stokes model, SCIPVIS. *AIAA Journal* 23(4), 505-514.
- Gamble, E., D. Terrell and R. DeFrancesco (2004). Nozzle selection and design criteria. *AIAA Paper* 3923, 1-11.
- Hassan, S., J. Masud and O. Khan (2015). *Intake and Airframe Characterization through Composite CFD*. 53rd AIAA Aerospace Sciences Meeting, AIAA SciTech Forum, (AIAA 2015-1669).
- Hirsch, C. (2007). *Numerical computation of internal and external flows: The fundamentals of computational fluid dynamics*, Butterworth-Heinemann.
- Jassim, E. I. (2016). CFD study on particle separation performance by shock inception during natural gas flow in supersonic nozzle. *Progress in Computational Fluid Dynamics*, 16(5), 300-312.
- Korst, H., R. White, S. E. Nyberg and J. Agrell (1981). Simulation and Modeling of Jet Plumes in Wind Tunnel Facilities. *Journal of Spacecraft and Rockets* 18(5), 427-434.
- Kuntz, M. and F. Menter (2004). Simulation of fluid-structure interactions in aeronautical applications. European Congress on *Computational Methods in Applied Sciences and Engineering*, Eccomas Jyväskylä, Finland.
- Li, G. and E. J. Gutmark (2005). Effect of exhaust nozzle geometry on combustor flow field and combustion characteristics. *Proceedings of the combustion institute* 30(2), 2893-2901.
- Li, W., R. Campbell, K. Geiselhart, E. Shields, S. Nayani and R. Shenoy (2009). Integration of Engine, Plume, and CFD Analyzes in Conceptual Design of Low-Boom Supersonic Aircraft. *AIAA Paper* 1171.
- Masud, J., A. Sayani and Z. Toor (2017). *Composite Analysis and Characterization of Exhaust Effects on Aerodynamic Behavior of a Supersonic Aircraft*. 55th AIAA Aerospace Sciences Meeting.
- Mattingly, J. D. and H. Von Ohain (2006). *Elements of propulsion: gas turbines and rockets*, American Institute of Aeronautics and Astronautics Reston, Va, USA.
- Mc Ghee, R. J. (1970). Jet-plume-induced flow separation on a lifting entry body at Mach numbers from 4.00 to 6.00. Technical Report NASA-TM-X-1997, L-6980.
- Mikhail, A. G., W. L. Hankey and J. S. Shang (1980). Computation of a supersonic flow past an axisymmetric nozzle boattail with jet exhaust. *AIAA Journal* 18(8), 869-875.
- Pandya, S. A., S. M. Murman and M. J. Aftosmis (2004). Validation of inlet and exhaust boundary conditions for a Cartesian method. *AIAA Paper* 4837, 2004.
- Rao, G. V. R. (1958). Exhaust nozzle contour for optimum thrust. *Journal of Jet Propulsion* 28(6): 377-382.
- Robinson, C. and M. High (1974). *Exhaust plume temperature effects on nozzle afterbody performance over the transonic Mach number range*, Arnold Engineering Development Center Arnold Afb Tn.
- Saddington, A. J., N. Lawson and K. Knowles (2004). An experimental and numerical investigation of under-expanded turbulent jets. *The Aeronautical Journal* 108(1081): 145-152.
- Stitt, L. E. (1990). Exhaust nozzles for propulsion systems with emphasis on supersonic cruise aircraft. Technical Report NASA-RP-1235.
- Virdi, P. S., M. S. Khan, N. Pereira, K. Suresh and R. S. D'Silva (2017). Design and Fabrication of Major Components of Turbojet Engine. *Energy and Power* 7(5), 130-135.
- Woodmansee, M. A., J. Dutton and R. P. Lucht (1999). *Experimental measurements of pressure, temperature, and density in an underexpanded sonic jet flowfield*. AIAA Fluid Dynamics Conference, 30 th, Norfolk, VA.